Animal Nutrition 11 (2022) 228–241

Contents lists available at ScienceDirect

Animal Nutrition

journal homepage: http://www.keaipublishing.com/en/journals/aninu/

Original Research Article

Chronic heat stress induces the disorder of gut transport and immune function associated with endoplasmic reticulum stress in growing pigs

Shanlong Tang [a, 1], Jingjing Xie [a, 1], Wei Fang [a, b], Xiaobin Wen [a], Chang Yin [a], Qingshi Meng [a], Ruqing Zhong [a], Liang Chen [a], Hongfu Zhang [a, *]

[a] State Key Laboratory of Animal Nutrition, Institute of Animal Science, Chinese Academy of Agricultural Sciences, Beijing, 100093, China
[b] Academy of State Administration of Grain, Beijing, 100037, China

ARTICLE INFO

Article history:
Received 16 January 2022
Received in revised form
6 August 2022
Accepted 11 August 2022
Available online 18 August 2022

Keywords:
Chronic heat stress
Gut transport and immunity
Endoplasmic reticulum stress
Growing pigs
Multi-omics

ABSTRACT

Although high temperatures influence gut health, data on underlying mechanisms remains scant. Using a pig model, this study performed a global analysis on how chronic heat stress affects the transport and immune function of the gut through transcriptome, proteome, microbial diversity and flow cytometry. A total of 27 pigs with similar body weights were assigned into 3 groups, control (Con) group (23 °C), chronic heat stressed (HS) group (33 °C), and pair-fed (PF) group, in a controlled environment for 21 days. Our results showed that pigs in the HS group had reduced growth performance and diminished height of ileal villi ($P < 0.01$). Transcriptome and proteome analyses demonstrated notable modification of expression of nutrients and ion transport-related transporters and gut mechanical barrier-related genes by chronic heart stress ($P < 0.05$), suggesting damage of transport functions and the gut barrier. Chronic heat stress-induced endoplasmic reticulum stress also increased the synthesis of misfolded proteins, leading to upregulation of misfolded protein degradation and synthesis, as well as vesicle transport disorder ($P < 0.05$). Energy supply processes were enhanced in the mitochondrion ($P < 0.05$) to maintain biological processes with high energy demands. Furthermore, chronic heat stress activated complement cascade response-related genes and proteins in the gut mucosa ($P < 0.05$). Our flow cytometry assays showed that the proportion of gut lymphocytes ($CD4^+$ T cells, T cells, B cells in Peyer's patch lymphocytes and $CD4^+$ $CD25^+$ T cells in intraepithelial lymphocytes) were significantly altered in the HS group pigs ($P < 0.05$). In addition, the occurrence of gut microbial dysbiosis in the HS group pigs was characterized by increased potential pathogens (e.g., *Asteroleplasma*, *Shuttleworthia*, *Mycoplasma*) and suppression of beneficial bacteria (e.g., *Coprococcus* and *Aeriscardovia*), which are associated with gut immune function. Altogether, our data demonstrated that chronic heat stress induced gut transport and immune function disorder associated with endoplasmic reticulum stress in growing pigs.

1. Introduction

The global temperature is rising at an unprecedented rate, and the frequency of heat waves is also increasing (Han et al., 2019). The Intergovernmental Panel on Climate Change (IPCC) predicts that the environmental temperature will rise by more than 4.8 °C over the coming 100 years, as a result of CO_2 emissions (Stocker, 2013). Previous data has demonstrated adverse effects exerted by ambient heat stress on the health of both humans and animals (Kovats and Kristie, 2006; Renaudeau et al., 2010). Continuous heat exposure has been shown to increase respiration rate and body temperature, slow weight gain and reduce ad libitum feed intake in animals (Pearce et al., 2013a; Rostagno, 2020; Xin et al., 2018). These shifts

* Corresponding author.
E-mail address: zhanghongfu@caas.cn (H. Zhang).
[1] These authors contributed equally to this work.
Peer review under responsibility of Chinese Association of Animal Science and Veterinary Medicine.

Production and Hosting by Elsevier on behalf of KeAi

https://doi.org/10.1016/j.aninu.2022.08.008

undoubtedly cause enormous annual economic losses to animal farming. Thus, with the rise in global environmental temperature, defining the mechanisms of heat stress-induced effects on animal health is important for sustainable development of animal husbandry. Vasoconstriction of the gastrointestinal tract induced by heat stress is a coordinated effort to support the thermoregulatory mechanisms of the body, shifting visceral blood flow towards peripheral circulation in an attempt to maximize radiant heat dissipation. Recent studies have examined the sensitivity of distinct organs to rises in body temperature, demonstrating that the resultant multi-organ failure, including the gastrointestinal tract, the central nervous system, the kidney, the liver and the muscle tissues, was closely associated with heat stress-induced cytotoxicity, coagulopathies and systemic inflammation (Fan et al., 2015; Heneghan et al., 2014; Littmann and Shields, 2016; Welc et al., 2013).

Since the gut is crucial for protecting against pathogens and the absorption of nutrients and immunity, it is susceptible to many stressors including heat, particularly in animals (Slawinska et al., 2019; Tellez et al., 2017). Because of decreased blood flood towards mesenteric circulation, the gut barrier is easily subjected to heat stress, which adversely affects the integrity of the intestinal epithelium (Lambert, 2009). Multiple in vitro and in vivo studies have demonstrated that heat stress weakens gut integrity and compromises gut barrier function, leading to a leaky gut (Cui and Gu, 2015; Varasteh et al., 2015). The heat-induced leaky gut enhanced translocation of bacteria endotoxins and antigens into the bloodstream, which in turn initiated an inflammatory response and cytokine production (including IL-6, IL-1beta and TNF-alpha) (Cui et al., 2019). Since the gut barrier can control uptake cross the mucosa, impaired intestinal integrity and function induced by heat stress was shown to cause preferential absorption of nutrients and led to unique alterations in post-absorptive metabolism, which were closely associated with both direct effects of high thermal loads and reduced caloric intake (Pearce et al., 2013c, 2015). In addition, microorganisms in mammals are associated with many gut physiological functions such as metabolism, immunity and nutrient absorption. Recent studies have reported that the composition and function of gut microbiota are altered by heat stress in poultry (Wang et al., 2018; Zhu et al., 2019). However, there is limited data on how heat stress influences the gut barrier, material transport and immune function.

The “omics” technologies, including transcriptomics, proteomics, and microbiomics, are indispensable high throughput methods with high precision and accuracy, and are widely used to study underlying mechanisms of environmental pollutants (such as ammonia, hydrogen, etc.) that threaten animal health (Liu et al., 2020; Tang et al., 2019, 2020). This study aimed to utilize multi-omics and flow cytometry tools to investigate the effects and mechanisms of chronic heat exposure on the gut barrier, transport of nutrients, immunophenotyping of gut-associated lymphoid tissue (GALT) as well as alterations of gut microbiota. Our findings provide convincing evidence on how chronic heat stress induces gut transport and immune function disorder, which offers critical insights into potential molecular mechanisms underlying its action, and also provides targets for nutritional intervention to reduce the adverse effects of heat stress.

2. Materials and methods

2.1. Animal ethic statement

This study received ethical approval from the Experimental Animal Welfare and Ethical Committee of Institute of Animal Science of Chinese Academy of Agricultural Sciences (IAS2018-5).

2.2. Animal management

Twenty-seven Large White male pigs (weighing 40.8 ± 2.7 kg) were individually kept in cages and randomly allocated into 3 treatment groups. Pigs in the control group (Con) were fed ad libitum at 23 °C in controlled climate chambers, while pigs in the chronic heat-stressed group (HS) were fed ad libitum at 33 °C. On the other hand, pigs from the pair-fed group (PF) were kept at 23 °C but provided with reduced amounts of feed equal to the HS pigs, implying that the volume of daily feed in the PF was equal to that consumed by the heat-stressed pigs the day before. The PF was thus used to adjust for the effects of reduced nutrient intake. All climate chambers were illuminated with a 16-h light cycle (light from 06:00 to 10:00) with a relative humidity of 55% ± 5%. Following the NRC (2012) requirement, the diet was primarily formulated by ground corn and soybean meal without any antibiotics (Table S1). After 7 d acclimatization in 23 °C controlled climate chambers, the pigs were subjected to respective treatments for 21 days before being euthanized by electric shock. To evaluate the state of heat stress, the respiration rate and rectal temperature of each pig was recorded weekly. To measure growth performance, initial and final body weight, as well as feed intake of each pig were recorded.

Pigs were euthanized by electric shock (Xingye Butchery Machinery Co. Ltd., Changde, China) and dissected by incision through the middle line of the abdomen. The intestines were immediately isolated and the last 10 cm of the ileum or whole cecum was dissected. The ileal and cecal sections were flushed with 50 mL physiological saline to remove the digesta. For morphological studies, 2 ileal and cecal rings were cut out and immersed in 4% freshly prepared paraformaldehyde. Pieces of ileal and cecal tissue were dissected and snap-frozen in liquid nitrogen for transcriptomics and proteomics analysis as well as qRT-PCR. The remaining ileal segments were opened up and Peyer's patches (PP) were separated according to characteristic morphology. The fresh ileal tissues and PP were transferred to a clean hood in the collection medium, which was used to isolate lymphocytes for flow cytometry. The collection medium was prepared with Ca^{2+}, Mg^{2+} free Hank's balanced salt solution (HBSS) with 20 IU/mL streptomycin and 0.01 M 4-(2-hydroxyethyl)-1-piperazineethanesulfonicaci (HEPES). The digesta in the ileum and cecum was aseptically collected in 2-mL tubes, and immediately put in liquid nitrogen and stored at −80 °C for sequencing of microbial 16s genes.

2.3. Intestinal morphology

Intestinal tissue blocks were fixed for 48 h. Dead tissue was carefully removed from each tissue block to make a 0.5 cm ileal or cecal loop. The ileal or cecal loop was then progressively dehydrated in more concentrated ethanol baths, followed by 100% xylene to remove ethanol. The dehydrated ileal or cecal tissue block was then embedded in paraffin wax, melted at 60 °C and then left at room temperature. The tissue-embedded paraffin blocks were kept at 4 °C before being sectioned into 5 μm thick slices. Thereafter, the slices were mounted onto glass slides in a 40 °C water bath and dried overnight in an oven at 37 °C. Before deparaffinization, the slices were heated in a 55 °C oven for 10 min. Thereafter, they were deparaffinized twice in xylene, followed by rehydration in a series of graded ethanol baths. The rehydrated slides were stained with filtered hematoxylin for 1 min, rinsed with distilled water and then re-stained with eosin for 30 s. The stained slices were again subjected to dehydration with graded ethanol baths and xylene, followed by application of a mounting medium and then covered with cover glass. Each section was analyzed under a light microscope. For each slide, the heights of 5 villi and the depths of 5 crypts were

recorded. In addition, the area of each PP nodule was recorded, followed by calculation of the total area of the PP and the average size of each nodule.

2.4. RNA sequencing analysis

Total RNA was isolated from the ileal tissue using TRIzol reagent (Invitrogen, Carlsbad, CA, USA) following the manufacturer's instructions. The integrity and purity of the total RNA was checked before construction of the sequencing library. The NEBNext Ultra RNA Library Prep Kit for Illumina (New England Biolabs, Ipswich, MA, USA) was used to generate the sequencing libraries, which were sequenced on an Illumina Hiseq platform (Illumina, San Diego, CA, USA) to generate paired-end reads. Thereafter, we used DESeq2 R package (1.18.1) to profile gene expression in the Con vs. HS and Con vs. PF. Differential expression genes (DEGs) were filtered based on a P-value < 0.01 and a fold-change ≥ 1.3 or ≤ 0.77. Further functional annotation and prediction analyses were implemented by DAVID (the Database for Annotation, Visualization and Integrated Discovery, version 6.8; https://david.ncifcrf.gov/summary.jsp) and Metascape enrichment analysis (https://metascape.org/gp/index.html#/main/step1). A P-value < 0.05 was considered as a significance threshold. The transcriptome analysis was performed as described by Tang et al. (2020).

2.5. Proteomics analysis

The SWATH 2.0 label-free quantitative proteomics technology was employed to analyze the whole proteome alterations associated with heat response of the pig ileum. Protein extraction and digestion from the ileum samples were performed as prescribed by the Filter Aided Sample Preparation (FASP) protocol. The digested peptides were collected for mass spectrometry analysis. The samples were analyzed through a reverse-phase high pressure liquid chromatography electrospray ionization tandem mass spectrometry (RP-HPLC-ESI-MS/MS) using a Triple TOF 6600 mass spectrometer (AB Sciex, Framingham, MA, USA) coupled to a nanoLC Eksigent 425 system (AB Sciex). The generation of SWATH-MS spectral library and qualitative and quantitative analysis of each protein was performed following a previously described protocol, Tang et al. (2015). After filtering the low quality of protein intensity, the t-test was used to analyze the protein expression in Con vs. HS and Con vs. PF. Differential expression proteins (DEPs) were assessed using a P-value < 0.05 and a fold-change ≥ 1.20 or ≤ 0.83. Further functional annotations and predictions were implemented by DAVID and Metascape enrichment analysis, with a P-value < 0.05 considered as the threshold of significance.

2.6. Microbiome analysis

Total bacterial DNA was extracted from the ileal and cecal digesta using the EZNATM Soil DNA kit (D5625-02, Omega Bio-Tek Inc., Norcross, GA, USA) following the manufacturer's instructions. The V3–V4 hypervariable regions of bacterial 16s rDNA were amplified via 2-step PCR analysis using a primer pair (338F and 806R), with unique 8 base pair barcodes to facilitate multiplexing. Sequencing was carried out with an Illumina sequencing platform using Miseq PE300. Raw data obtained from the gut microbiota were processed using Majorbio I-Sanger Cloud Platform (www.i-sanger.com), and then redundant sequences were filtered. UPARSE (version 7.1, http://drive5.com/uparse/) was used to cluster the operational taxonomic units (OTUs) at a 97% similarity cutoff, and each representative OTU was mapped to Silva 138 database by an RDP classifier (http://rdp.cme.msu.edu/) using a confidence threshold of 0.7. The principal co-ordinates analysis (PCoA) was performed using Majorbio I-Sanger Cloud Platform, and significant difference among any 2 of the 3 distinct groups at genus level was tested using the DESeq2 method (MicrobiomeAnalyst, https://www.microbiomeanalyst.ca/) with a P-value < 0.05.

2.7. Flow cytometry analysis of the gut-associated lymphoid tissue (GALT)

To isolate intraepithelial lymphocytes (IEL) from the ileum, a 30-mL HBSS-dithiothreitol (DTT) solution (0.01 M HEPES; 2 mM DTT) was added into a fresh ileal tissue, and then incubated in a 37 °C water bath for 5 min. Thereafter, tissues were then transferred into a 25-mL HBSS-EDTA solution (made of Ca^{2+}, Mg^{2+} free HBSS with 3 mM EDTA and 0.01 M HEPES), and incubated for 45 min at 37 °C. The HBSS-EDTA was passed through a 70-μm filter and then the flow-through solution containing IEL was kept on ice. Each ileal tissue was subjected to a second 45 min incubation in the 25-mL HBSS-EDTA solution. The 2 filtered solutions were pulled and centrifuged at 600 × g for 10 min. The pelleted cells were resuspended in 1-mL RPMI-1640 medium for flow cytometry analysis (the details of antibodies seen in Table S2).

To isolate the ileal PP lymphocytes (PPL) from the ileum, the ileal tissue was incubated in 30 mL HBSS-DTT solution for 30 min in a 37 °C water bath, and then incubated in a 25 mL HBSS-EDTA solution for 30 min. The PP was cut into small pieces and ground on a 70-μm screen with 6 mL HBSS-EDTA solution. The filtrate was collected into a 15 mL conical tube and then the PPL was pelleted by centrifugation at 600 × g for 10 min. The cells were rinsed with 10 mL RPMI-1640 medium and then resuspended in 1 mL RPMI-1640 medium for flow cytometry analysis.

2.8. Specific gene expression analysis by qRT-PCR

Total RNA was isolated from the ileum and cecum using TRIzol reagent (Invitrogen, Carlsbad, CA, USA), following the manufacturer's instructions. The concentration of each RNA sample was determined by a NanoDrop 2000 (Nanodrop Technologies, Wilmington, DE, USA). Before reverse transcription, genomic DNA contamination was removed by incubation of the RNA with gDNA Eraser in the PrimeScript RT reagent kit (Takara, Shige, Japan). We conducted qRT-PCR using a commercial kit (SYBR Premix Ex TaqTM, Takara). The specificity of each primer (Table S3) set was verified by a single peak in the melting curves after 40 PCR amplification cycles. Relative expression of targeted genes that code for tight junction proteins and other genes between different groups was calculated by the $2^{-\triangle\triangle Ct}$ method using *β-actin* as the reference gene.

2.9. Statistical analysis

The data obtained from the growth performance, intestinal morphology, relative gene expression, bacterial alpha-diversity indices and flow cytometry analysis were analyzed by one-way ANOVA using the JMP software (JMP version 10.0.0, SAS Institute, Cary, NC, USA). The Student's multiple comparisons t-test was used to compare results between every 2 of 3 distinct groups. The data from rectal temperature and respiration rate over time were analyzed by repeated measures using an autoregressive covariance method. The treatment, day and their interaction were used as fixed effects, while the data collected on d 0 was used as covariance. The Spearman's correlation analysis between immunophenotyping of IEL or PPL and cecal differential microbes was executed by the ggcor R package. A P < 0.05 was considered as statistically significant, while 0.05 < P < 0.10 was set as a significant trend.

3. Results

3.1. Growth performance and intestinal morphology

The results as described by Xin et al. (2018) showed that compared with the Con pigs, the HS pigs had a dramatic increase in rectal temperature and almost a 2.5-fold increase in overall respiration rate, whereas the rectal temperature and respiration rate decreased in the PF pigs ($P < 0.01$, Fig. 1A and B). Exposure to 33 °C significantly suppressed the average daily feed intake of the pigs by 44.9%, average daily body weight gain by 62.2% and end body weight by 18.4% compared with the Con pigs, while there was low average daily body weight gain and end body weight in PF pigs ($P < 0.0001$, Fig. 1C, D and E).

Further analysis of intestinal morphology revealed that villi height of the ileum was approximately 25% shorter in the HS and PF pigs compared to that in the Con pigs ($P < 0.0001$, Fig. 1F and G). Ileal crypt depth tended to be increased in the HS pigs ($P = 0.0968$, Fig. 1F and H), but not in the cecum, which was comparable with the other 3 groups ($P = 0.6636$, Fig. 1F and J). In addition, the V/C (villi height/crypt depth) ratio of the ileum was also significantly reduced in the HS and PF pigs compared to the Con pigs ($P = 0.0002$, Fig. 1F and I).

Gene expression analysis in the tight junction protein illustrated that claudin-4 expression had a downward trend in the HS pig ileum ($P = 0.0818$, Table S4). There were, however, no changes in the expression of *ZO-1*, occludin, claudin-1, claudin-3 in ileum and *ZO-1*, occludin, claudin-1, claudin-3, claudin-4 in the cecum ($P > 0.05$, Table S4).

3.2. Ileal transcriptome

After quality control and mapping of the sequences from the RNA-Seq, DEGs were filtered using the DESeq2 method. As shown in Supplementary file 1, a total of 468 DEGs (*P*-value < 0.01, fold-change ≥ 1.3 or ≤ 0.77) were filtered in the ileal mucosa of pigs exposed to 33 °C (Con vs. HS), which included 69 new genes and 348 annotated genes. In the pair-fed group, 124 DEGs were observed (*P*-value < 0.01, fold-change ≥ 1.3 or ≤ 0.77) with 30 new genes and 82 annotated genes (Con vs. PF). A total of 32 common DEGs were shared between the Con vs. HS and Con vs. PF (Fig. 2A and D). Out of the total, there were 31 common DEGs in the HS and PF pigs compared to the Con pigs, and only one common DEG (*A4GNT*, number 32) was up-regulated in the HS and down-regulated in the PF. Therefore, 437 exclusive DEGs (including *A4GNT*) in the HS were filtered, which included 122

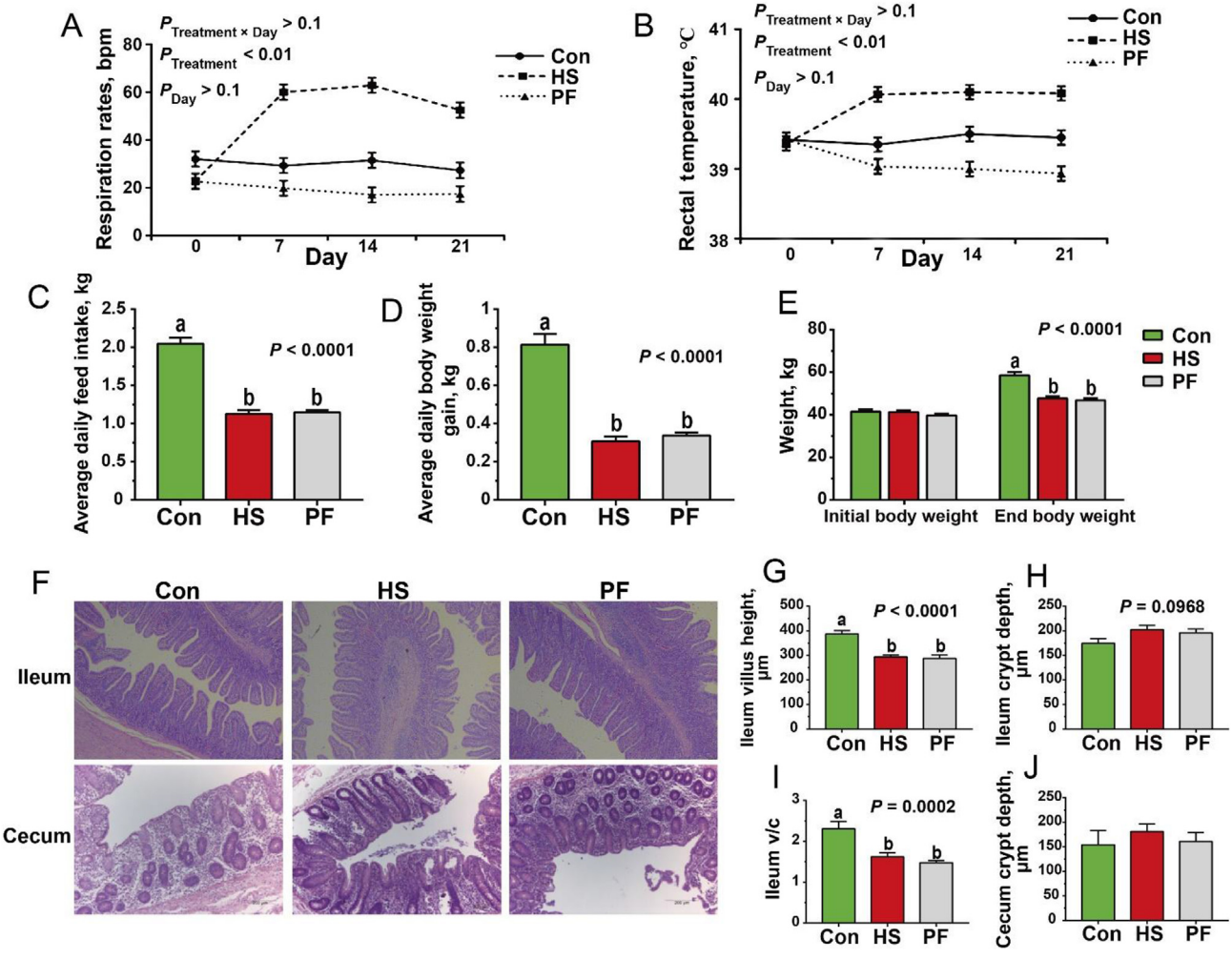

Fig. 1. Growth performance and intestinal morphology. (A) The respiration rate and (B) rectal temperature of pigs in 3 groups; (C) the average daily feed intake, (D) average daily body weight gain, (E) initial body weight and end body weight in each group of pigs; (F) the H&E staining of the ileum and cecum; (G) the villus height, (H) crypt depth, and (I) V/C of ileum, as well as (J) crypt depth of cecum. Data are presented as mean ± SE ($n = 9$) and different letters indicate significant differences among groups at $P < 0.05$. bpm = breaths per minute; Con = control group; HS = heat stress group; PF = pair-fed group; V/C = villi height-to-crypt depth ratio.

up-regulated genes and 315 down-regulated genes (Fig. 2B). To validate the RNA-seq results, qRT-PCR analysis was conducted and yielded results that were consistent with the RNA-Seq findings (Fig. S1).

We performed pathway enrichment analysis for the exclusive DEGs in the Con vs. HS. KEGG pathway analysis by DAVID revealed that there was marked enrichment of DEGs in pathways related to nutrient absorption and transport (ssc04974: protein digestion and absorption, ssc04973: carbohydrate digestion and absorption, ssc00040: pentose and glucuronate interconversions), phospholipid metabolism (ssc00564: glycerophospholipid metabolism, ssc00140: steroid hormone biosynthesis), actin cytoskeleton (ssc04810: regulation of actin cytoskeleton) and signaling (ssc04350: TGF-beta [Transforming growth factor-beta] signaling pathway, ssc04012: ErbB [epidermal growth factor receptor] signaling pathway, ssc04912: GnRH [Gonadotropin-releasing hormone] signaling pathway) ($P < 0.05$, Fig. 2C and Supplementary file 2). Metascape enrichment network analysis demonstrated that DEGs were mainly enriched in intestinal transport (R-HAS-382551: transport of small molecules; GO: 0006820, anion transport; GO: 0015893, drug transport; GO: 0070633, transepithelial transport), lipid metabolism (GO: 0010876, lipid localization; GO: 0032787, monocarboxylic acid metabolic process; R-HAS-174824: plasma lipoprotein assembly, remodeling and clearance; GO: 0006654, phosphatidic acid biosynthetic process; GO: 0055088, lipid homeostasis) and response to hypoxia (GO: 0001666, response to hypoxia; GO: 0000302, response to reactive oxygen species) ($P < 0.01$, Fig. 2E and Supplementary file 2).

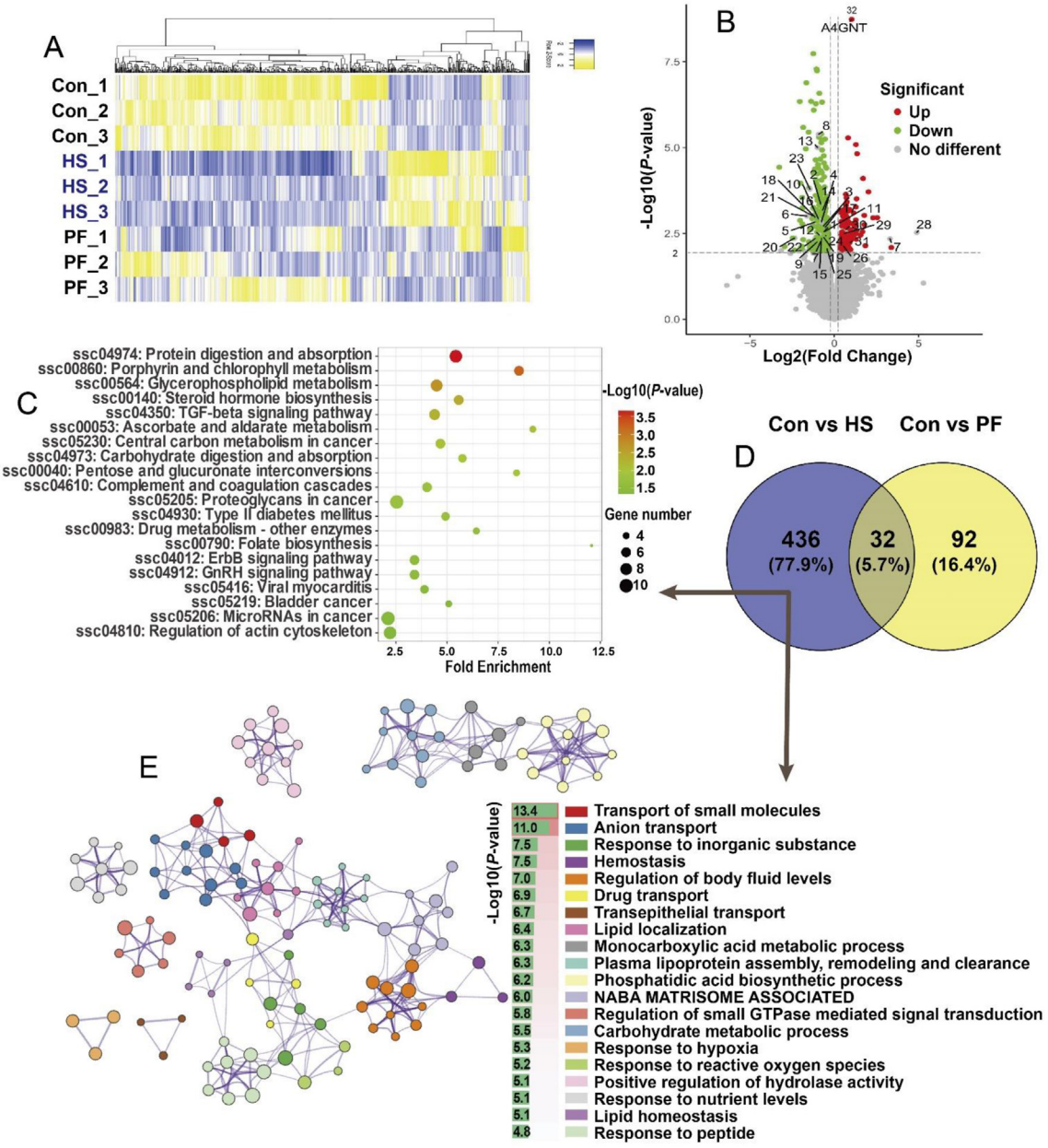

Fig. 2. The ileal transcriptome profiles ($n = 3$). (A) The heat map of relative expression level (FPKM); (B) volcano plot for exclusive DEGs (including *A4GNT*) in Con vs. HS; (D) Venn diagram between Con vs. HS and Con vs. PF; (C) the KEGG pathway analysis and (E) Metascape enrichment network for exclusive DEGs in Con vs. HS. Con = control group; HS = heat stress group; PF = pair-fed group; A4GNT = alpha-1,4-N-acetylglucosaminyltransferase; KEGG = Kyoto Encyclopedia of Genes and Genomes; DEGs = differential expression genes.

3.3. Ileal proteomics

After filtering of low quality protein intensity, DEPs were determined by the *t*-test method in the HS and PF ($P < 0.05$, fold change >1.2 or < 0.833). A total of 117 DEPs were identified in the ileal mucosa of the HS and Con pigs, which included 22 down-regulated proteins and 95 up-regulated proteins (Fig. 3A and Supplementary file 3). There were 69 DEPs in the PF and Con pigs, which included 37 down-regulated and 32 up-regulated proteins (Fig. 3A and Supplementary file 3). There were a total of 8 common DEPs in the Con vs. HS and Con vs. PF (Fig. 3A and D). Among these, there was high consistency in 7 common DEPs (up- or down-regulated) in the HS and PF pigs compared to Con pigs, and only one common DEP (ACLY) was up-regulated in the Con vs. HS and down-regulated in Con vs. PF. Therefore, 110 exclusive DEPs were filtered in the Con vs. HS, which included 92 up-regulated and 18 down-regulated proteins (Fig. 3B).

The DAVID and Metascape databases were utilized for further pathway enrichment analysis for the exclusive DEPs in the Con vs. HS. KEGG pathway analysis by DAVID demonstrated that the DEPs were notably enriched in pathways related to citrate cycle (TCA cycle, ssc00020), carbon metabolism (ssc01200), degradation of aromatic compounds (ssc01220), protein processing in the endoplasmic reticulum (ssc04141) and metabolic pathways (ssc01100) ($P < 0.05$, Fig. 3C and Supplementary file 4). In addition, the Metascape enrichment network showed that the DEPs were mainly enriched in protein folding, localization and degradation (GO: 0006457, protein folding; GO: 0090150, establishment of protein localization to membrane; GO: 0042026, protein refolding; GO: 1903362, regulation of cellular protein catabolic process; R-HAS-71291: metabolism of amino acids and derivatives), intracellular transport (GO: 0045055, regulated exocytosis; R-HAS-5653656, vesicle-mediated transport), regulation of innate immune response (GO: 0045088) and

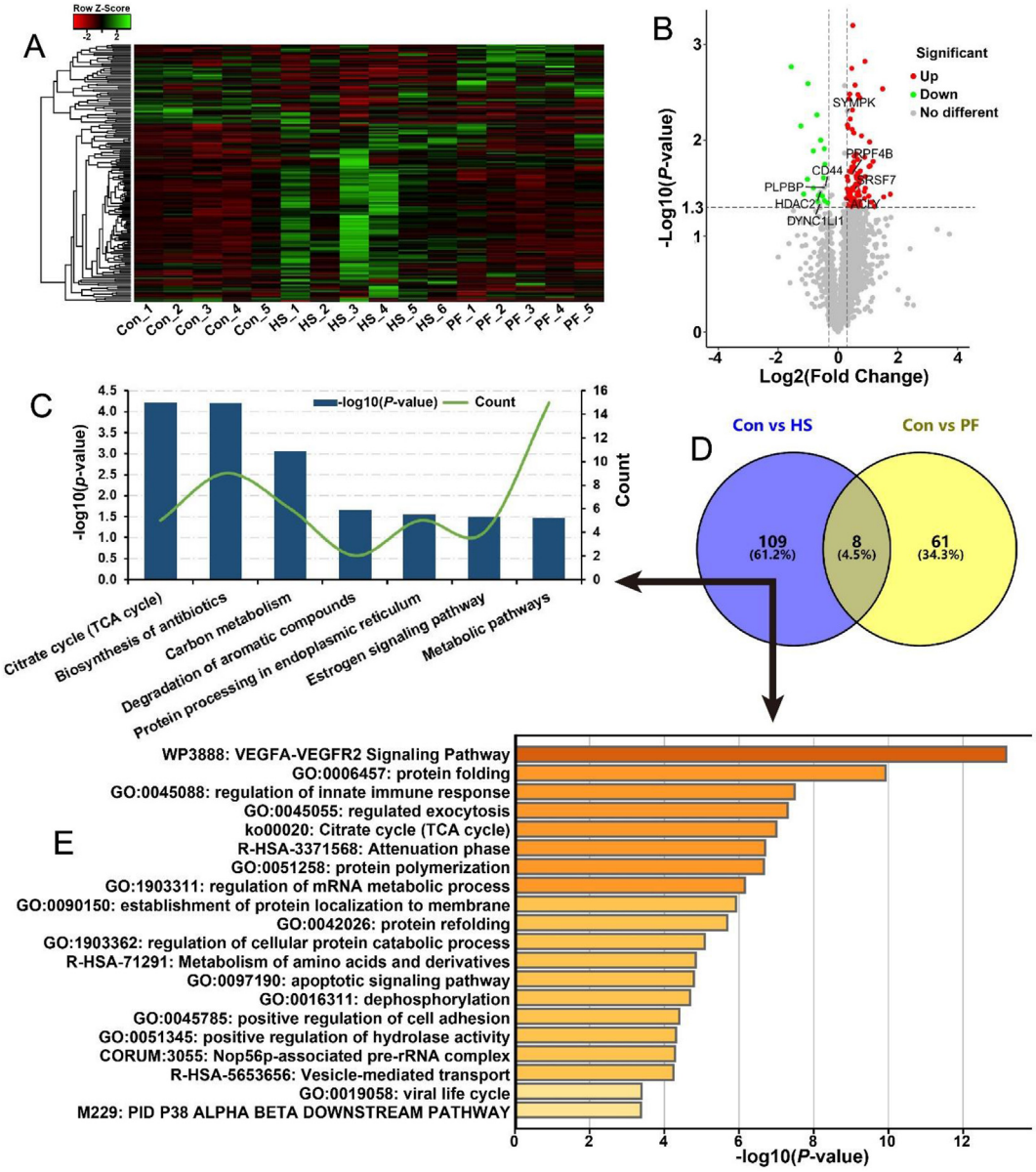

Fig. 3. The ileal proteomics profiles ($n = 5$ to 6). (A) The heat map of hierarchical cluster analysis for DEPs; (B) volcano plot for exclusive DEPs (including ACLY) in Con vs. HS; (D) Venn diagram between Con vs. HS and Con vs. PF; (C) the KEGG pathway analysis and (E) Metascape enrichment analysis for exclusive DEPs in Con vs. HS. Con = control group; HS = heat stress group; PF = pair-fed group; ACLY = ATP-citrate synthase; KEGG = Kyoto Encyclopedia of Genes and Genomes; DEPs = differential expression proteins.

positive regulation of cell adhesion (GO: 0045785) ($P < 0.01$, Fig. 3E and Supplementary file 4).

3.4. Immunophenotyping analysis for gut-associated lymphoid tissue (GALT)

To further understand how heat stress influences ileal immunity, we profiled and analyzed the ileal GALT (IEL and PPL) immune cells and the PP area. As shown in Fig. 4A–C, the size of the lymphoid nodule in the PP was significantly lower in the HS pigs compared with the Con pigs ($P = 0.0441$, Fig. 4A and C). However, the PP area did not markedly differ among the 3 distinct groups ($P > 0.05$, Fig. 4A and B). There was also no notable alteration in the $CD3^+$ $CD8^+$ cells, $CD3^+$ $CD4^-$ $CD8^-$ cells and $CD3^+$ $CD4^+$ $CD25^+$ cells among the 3 groups ($P > 0.05$, Fig. 4G–I and D). The heat-stressed pigs displayed an upward trend of $CD3^+$ $CD4^+$ cells compared with the Con pigs ($P = 0.0855$, Fig. 4F and D). Heat stress increased the T cell ratio ($P = 0.0418$, Figs. S2B and A) and suppressed the B cell ratio ($P = 0.0193$, Figs. S2C and A) in the pig's PPL compared with the Con pigs. The ratio of T cells to B cells was significantly improved in the HS pig's PP compared with the Con or PF pigs ($P < 0.0001$, Figs. S2I and A). Compared with the Con pigs, there was no significant change in the activated T cells ($CD3^+$ SLA-DR^+ cells; Fig. S2D and A), $CD3^-$ $CD21^-$ $CD14^+$ cells (Figs. S2E and A), NK cells ($CD3^-$ $CD21^-$ $CD14^-$ SLA-DR^- cells, Figs. S2F and A) or $CD3^-$ $CD21^-$ $CD14^-$ SLA-DR^+ cells (Figs. S2G and A) and there was an upward trend in activated B cells ($CD3^-$ $CD21^+$ SLA-DR^+; $P = 0.0974$, Figs. S2H and A) in the HS pig's PP.

In the IEL, the $CD3^+$ $CD4^+$ $CD25^+$ cells were significantly lower in the HS pigs compared with those in the Con pigs ($P = 0.0256$, Figs. S3F and A). There were no marked differences in $CD3^+$ $CD4^+$ cells, $CD3^+$ $CD8^+$ cells and $CD3^+$ $CD4^-$ $CD25^+$ cells among the 3 different groups ($P > 0.05$, Figs. S3C-E). Similarly, there was no obvious change in T or B cells, NK cells, activated T or B cells, $CD3^-$ $CD21^-$ $CD14^+$ cells and $CD3^-$ $CD21^-$ $CD14^-$ SLA-DR^+ cells in the pig's IEL across the 3 distinct groups ($P > 0.05$, Figs. S4A–H).

3.5. Ileal and cecal microbiome

Our analysis showed that the alpha-diversity (Shannon or Chao index) of the ileal samples did not show significant differences at any taxonomic levels with or without heat stress ($P > 0.05$, Fig. 5A and B). PF pigs had higher microbial richness in the cecum at all taxonomic levels (except for OTU level), compared to the Con pigs as demonstrated by Chao and Shannon index ($P < 0.05$, Fig. 5A and B). In addition, the Chao index showed that heat stress only increased microbial richness at phylum level in the cecum compared to the Con pigs ($P = 0.0201$, Fig. 5B). PCoA based on Bray–Curtis distance demonstrated that there was no clear cluster of the microbial community at OTU level in the ileal (Adonis $R^2 = 0.1288$, $P = 0.3210$, Fig. 5C) or cecal (Adonis $R^2 = 0.1473$, $P = 0.1830$, Fig. 5D) contents in the 3 different groups.

The composition of the microbial community mainly contained 5 major phyla, including Firmicutes, Proteobacteria, Actinobacteriota, Campilobacterota and Bacteroidota, which accounted for more than 99.5% of the total phyla in the ileum. There was no obvious difference at the phylum level after heat stress or feeding restriction. In contrast, the most abundant phyla in the cecum were Bacteroidota (60.01%) and Firmicutes (37.34%), which consisted of approximately 99.8% of the total phyla while Cyanobacteria, Campilobacterota, Proteobacteria and Spirochaetota accounted for 0.85%, 0.95%, 0.49% and 0.16%, respectively. Heat stress significantly decreased the relative abundance of Bacteroidota ($P = 0.0111$) at the phylum level, while feeding restriction notably increased the Synergistota ($P = 0.0086$) and Spirochaetota ($P = 0.0137$) (Fig. 5I and Supplementary file 5). The major genera abundance (more than 1%) from each group in the ileum or cecum was shown in Fig. 5E or Fig. 5G. In addition, our analysis identified a total of 6 genera in the ileal digesta of pigs exposed to 33 °C (Con vs. HS), which included 3 down-regulated genera (*Escherichia_Shigella, Clostridium_sensu_stricto_6* and *Aeriscardovia*) and 3 up-regulated genera (*Mycoplasma*, *norank_f_Erysipelotrichaceae* and Prevotellaceae_*NK3B31_group*) ($P < 0.05$, Fig. 5F and Supplementary file 5). In the ileal digesta of the PF pigs, there were 5 identified genera, which included 3 down-regulated genera (*Faecalibacterium*, *Intestinibacter* and *Clostridium_sensu_stricto_6*) and 2 up-regulated genera (*Cellulosilyticum* and *Phascolarctobacterium*) ($P < 0.05$, Fig. 5F and Supplementary file 5). In the cecum digesta, heat stress increased genera *Asteroleplasma*, *Shuttleworthia*, *Intestinimonas*, *Turicibacter*, *Desulfovibrio Clostridium_sensu_stricto_1* and decreased genera *Coprococcus*, *Lachnospiraceae_UCG_004*, *Defluviitaleaceae_UCG_011*, *Eubacterium_xylanophilum_group*. The feeding restriction increased genera *Bacteroides*, *Sphaerochaeta*, *dgA_11_gut_group*, *Eubacterium_siraeum_group*, *norank_f_Bacteroidales_RF16_group*, *unclassified_c_Bacteroidia*, *Treponema*, *Lachnospiraceae_NK4A136_group*, *Parabacteroides*, *Pyramidobacter*, *Clostridium_sensu_stricto_1*, *Asteroleplasma* and decreased genera *Anaerostipes*, *Lactobacillus*, *norank_f_Prevotellaceae*, Prevotellaceae_*UCG_003*, and *Alloprevotella* ($P < 0.05$, Fig. 5H and Supplementary file 5).

4. Discussion

Studies have shown that ambient heat stress has negative effects on animal health (Kovats and Kristie, 2006; Renaudeau et al., 2010). The current results demonstrated that pigs exposed to 33 °C developed significant heat stress, as evidenced by the increase in respiration rate and temperatures and decrease in feed intake and body weight, which was consistent with previous studies (Pearce et al., 2013a, 2014; Seelenbinder et al., 2018). The main explanation for the diminished growth performance was that heat stress impaired gut morphology which lead to light shedding of the intestinal mucosa, due to the reduced feed intake induced by heat exposure. These phenomena have been reported previously (Cui and Gu, 2015; Koch et al., 2019; Pearce et al., 2013c, 2014; Rostagno, 2020). Several studies found that heat exposure caused gut barrier dysfunction and hyperpermeability via reducing the expression and distribution of tight junction (TJ) proteins (Hall et al., 2001; Yang et al., 2007). The expression of primary TJ proteins in pigs was decreased at 3 days of heat exposure (Xia et al., 2022), and increased at 7 days of heat exposure (Xiong et al., 2022), but expression was not altered at 21 days of heat stress in this present trail. This might be due to the compensatory repair of intestinal TJ proteins mediated by heat shock proteins (HSPs) in response to heat exposure (Dokladny et al., 2006, 2008; Pearce et al., 2013b). Nevertheless, our transcriptome data revealed that the mechanical barrier-related genes (including *CLDN4*, *CXADR*, *KRT20* and *ALP*; Fig. 6C) in the ileum were remarkably down-regulated by heat exposure independent of the reduced feed intake. The coxsackievirus and adenovirus receptor (CXADR) and KRT20 (keratin 20), the major intermediate filament proteins in the intestinal epithelia, regulate the epithelial TJ integrity (Cui and Gu, 2015; Oliveto et al., 2018). Glycosylation contributes to the maintenance of the intestinal barrier (Nagao-Kitamoto et al., 2020) and glycosylation-related genes (*MGAT4A* and *A4GNT*; Fig. 6C) were also altered in the ileum of HS pigs. These findings indicated that heat stress had negative effects on barrier function and morphology in the porcine ileum, leading to a reduction in growth performance in growing pigs.

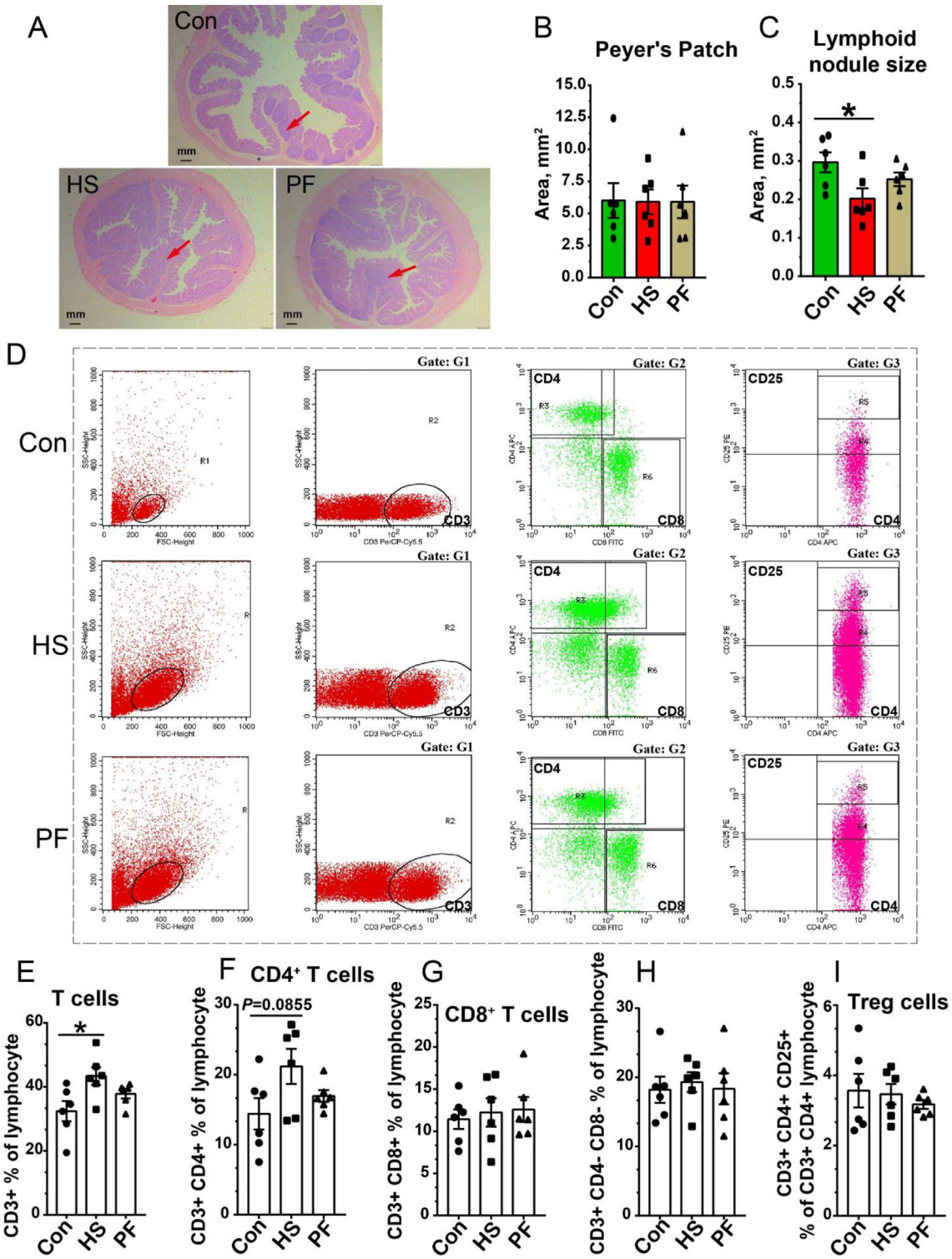

Fig. 4. The immunophenotyping of T lymphocytes in ileal PP ($n = 6$). (A) The H&E staining of ileal PP, and (B) the area of PP as well as (C) the size of its internal lymphoid nodule among 3 groups; (D) the representative plot of T lymphocytes and proportion analysis of various type of cells including T cells (E), $CD3^+$ $CD4^+$ cells (F), $CD3^+$ $CD8^+$ cells (G), $CD3^+$ $CD4^-$ $CD8^-$ cells (H) and $CD3^+$ $CD4^+$ $CD25^+$ cells (F) in ileal PP from Con, HS and PF pigs by flow cytometry. Asterisk denotes significant differences ($^*P < 0.05$), and data are represented as mean ± SE. The red arrow denotes the ileal PP. Con = control group; HS = heat stress group; PF = pair-fed group; PP = Peyer's patch. (The gate strategy of flow cytometry seen in Fig. S6).

Furthermore, transcriptome sequencing showed that chronic heat exposure altered the expression of genes related to nutrient absorption (such as carbohydrate, amino acid and peptide) in the pig intestine, independent of the reduced feed intake. Moreover, heat stress down-regulated the expression of glucose transporters *GLUT2* (*SLC2A2*) and *SGLT1* (*SLC5A1*) in pigs (Fig. 6G and H). By contrast, it was earlier reported that short-term heat exposure up-regulated expression of glucose transporters (Pearce et al., 2013b),

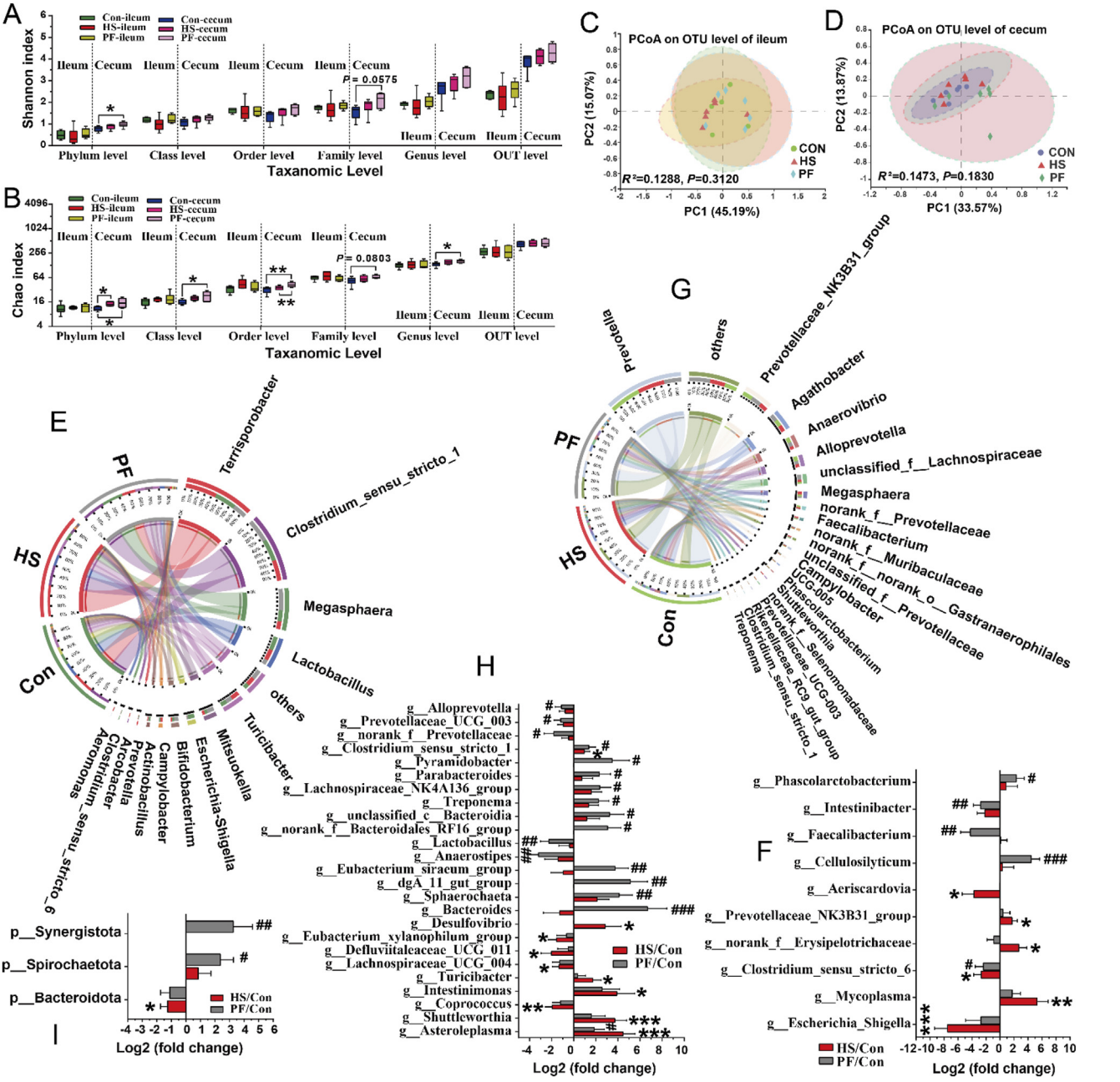

Fig. 5. Microbiome analysis. (A) Shannon or (B) Chao index among 3 groups; principal co-ordinate analysis (PCoA, OTU level) of community membership based on Bray–Curtis distance in the ileum (C) and cecum (D); The mainly enriched genera from the ileum (E) and cecum (G) in Con vs. HS or PF; the differentially abundant genera from the ileum (F) and cecum (H) after heat stress or restricted feeding; (I) the differentially abundant phyla from the cecum in Con vs. HS or PF. * or # indicates different at $P < 0.05$, ** or ## indicates significant different at $P < 0.01$ and *** or ### indicates significant different at $P < 0.001$. Con = control group; HS = heat stress group; PF = pair-fed group; PP = Peyer's patch.

indicating that short-term and long-term heat stress may act through different routes. Consistent with a previous study (Li et al., 2013), our study shows that chronic heat stress reduced the transport of cationic amino acids and small peptides in the gut, but it increased the expression of neutral amino acid transmembrane transporters (*ASCT2* [*SLC1A5*] and *4F2hc* [*SLC3A2*]) (Fig. 6E and F). Morales et al. (2016) reported that exposure to heat affected the amino acid composition of endogenous intestinal proteins in growing pigs, resulting in increased loss of endogenous intestinal proteins and amino acids. Therefore, the retention of neutral amino acid transporters in the gut under heat exposure condition may be the body's survival defense mechanism, but the specific reasons still need to be further explored. Overall, chronic heat exposure impaired the transport of glucose and protein in the intestine, which partly explains the reduction in growth performance.

In addition, transcriptional and proteomic data showed that chronic heat exposure markedly interfered with the intestinal transport of water, lipids (including glycerol), nucleosides, vitamins, glucosamine, inorganic/metal ions, and amino acids across mitochondrial membrane in growing pigs (Fig. 6I-L). Membrane transporters mainly include members of the ion and water channels, ATP-binding cassette (ABC) and solute carrier (SLC) transporters (Zhang

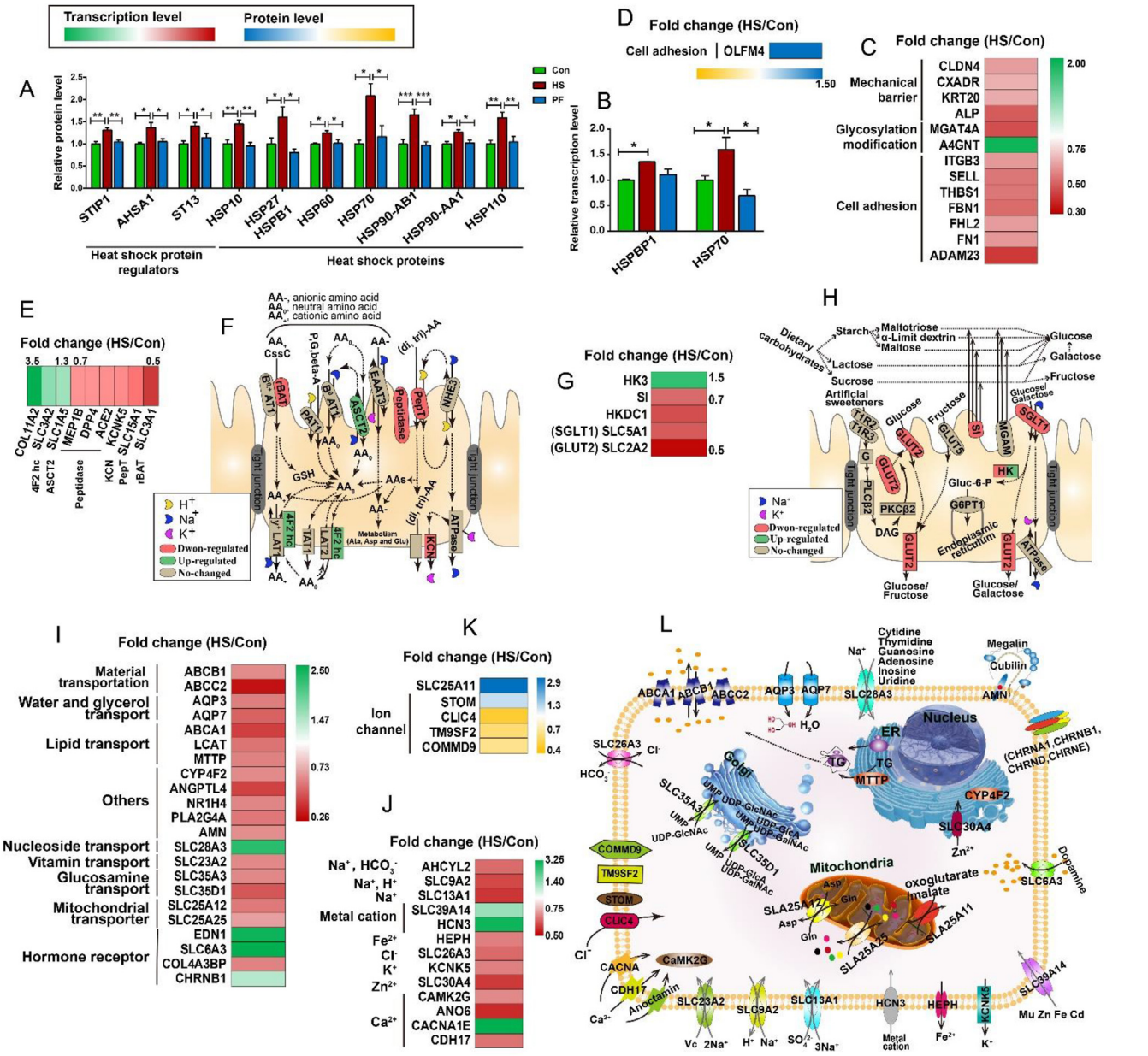

Fig. 6. Transcriptomics and proteomics revealed that intestinal barrier and substance transport were damaged under conditions of chronic heat stress in growing pigs. The effect of heat stress on the expression of heat shock protein in protein level (A) or transcription level (B). Fold change of differentially expressed genes or proteins related to protein (E) or carbohydrate (G) absorption and the intestinal barrier (C and D); the process of heat stress-induced protein (F) or carbohydrate (H) absorption disorder. Fold change of differentially expressed genes or proteins related to the transport of small molecules (I) or ions (J and K); (L) the process of heat stress-induced transport disorder of small molecules or ions. * and ** indicates different at $P < 0.05$ and 0.01. (Full name of differential expression genes or proteins seen in supplementary file 1 or 3).

et al., 2019). The expression of these transporters was altered by chronic heat exposure. The impaired ion transport affected the transport of substances in the intestine, especially the absorption of nutrients, decreased the intestinal epithelial barrier function, and affected the acid-base balance in the intestinal lumen and intestine. The transport and secretion of intestinal bicarbonate is a critical nonstructural mechanism that protects against alterations in luminal pH (Kiela and Ghishan, 2009). Several essential transporters (such as Na^+/HCO_3^- cotransporter, Na^+/H^+ exchangers, Cl^- channel) participate in this defense mechanism. Several intestinal inflammation and inflammatory mediators influence the expression and function of vital epithelial transporters (for example Na^+/K^+ ATPase, $Na^+/K^+/Cl^-$ cotransporter 1, Na^+/H^+ exchangers, epithelial Na^+ channel), and thus regulate fluid homeostasis and occurrence of diarrhea (Kiela and Ghishan, 2009). Therefore, heat exposure will disrupt intestinal transport systems, hence damaging gut health. The transport of calcium, a vital intracellular messenger that regulates various cellular processes such as cell proliferation and apoptosis, was affected by chronic heat exposure as indicated by changes to the expression of calcium-related transporters. These findings demonstrated that heat stress directly and indirectly affected intestinal transport dysfunction.

The consequence of the mismatch between the load of unfolded and misfolded proteins in the endoplasmic reticulum (ER) and capacity of the cellular machinery that copes with that load is called ER stress (Ron and Walter, 2007). ER stress is caused by several stimuli, both from the inside and outside of cells. Molecular chaperones (such as HSPs), which are mainly present in the ER, can be

used as marker proteins of ER stress (Gotoh et al., 2011). Previous studies showed that exposure to environmental challenges increased the expression of HSPs (Chi et al., 2018; Sun et al., 2016). In the present study, chronic heat exposure dramatically increased the expression of HSPs (especially HSP 70 and 90) and HSP regulatory proteins in pig ileum (Fig. 6A and B), indicating that heat stress may cause intestinal ER stress. Analysis of the proteomic data in this study revealed that chronic heat exposure increased protein-folding errors in intestinal epithelial cells, causing ER stress. An important process for preventing protein misfolding and excessive accumulation of misfolded proteins is the ubiquitin-proteasome pathway. In the present study, the expression of ubiquitin-conjugating enzymes (E2, including UBE2L6 and UBE2V2), ubiquitin ligases (E3, including TRIM31 and TRIM21), calcyclin-binding protein (CACYBP), and proteasome activator subunit 1 (PSME1) was increased (Fig. 7G and H). However, this self-regulation and defense mechanism did not limit the rate of protein synthesis, as evidenced by the increased proteins related to protein synthesis (Fig. 7G and H) and protein sorting (Fig. 7E and H). The increase in protein synthesis and sorting processes might be a negative feedback mechanism to decrease protein end-products due to increased protein-folding caused by ER stress following chronic heat exposure. The increased error rate of protein-folding induced by heat stress enhanced high energy-demand biological processes such as protein synthesis, sorting and degradation, leading to excessive energy waste. Analysis of proteomic data showed that the expressions of protein involved in glycogen degradation, fatty acid oxidation and TCA cycle-related enzymes were increased in intestines of HS pigs (Fig. 7D and H), indicating increased mitochondrial energy production to meet biological process with high energy requirements. Given the impaired glucose absorption in the gut, augmentation of mitochondrial energy production induced by chronic heat exposure was likely to induce intestinal energy failure. One interesting finding regarding intestinal vesicle transport was the extent to which chronic heat stress restricted the expression of membrane fluidity and vesicular protein-related genes and increased the expression of vesicle docking and localization-related proteins in pig ileum (Fig. 7E, F and H). This contradictory result made it difficult to evaluate the effect of chronic heat stress on vesicle transport in intestinal epithelial cells. Nevertheless, the results showed that chronic heat stress disrupted vesicle transport in intestinal epithelial cells.

The intestine plays an important role in digestion and absorption of nutrients and is also the most extensive barrier organ

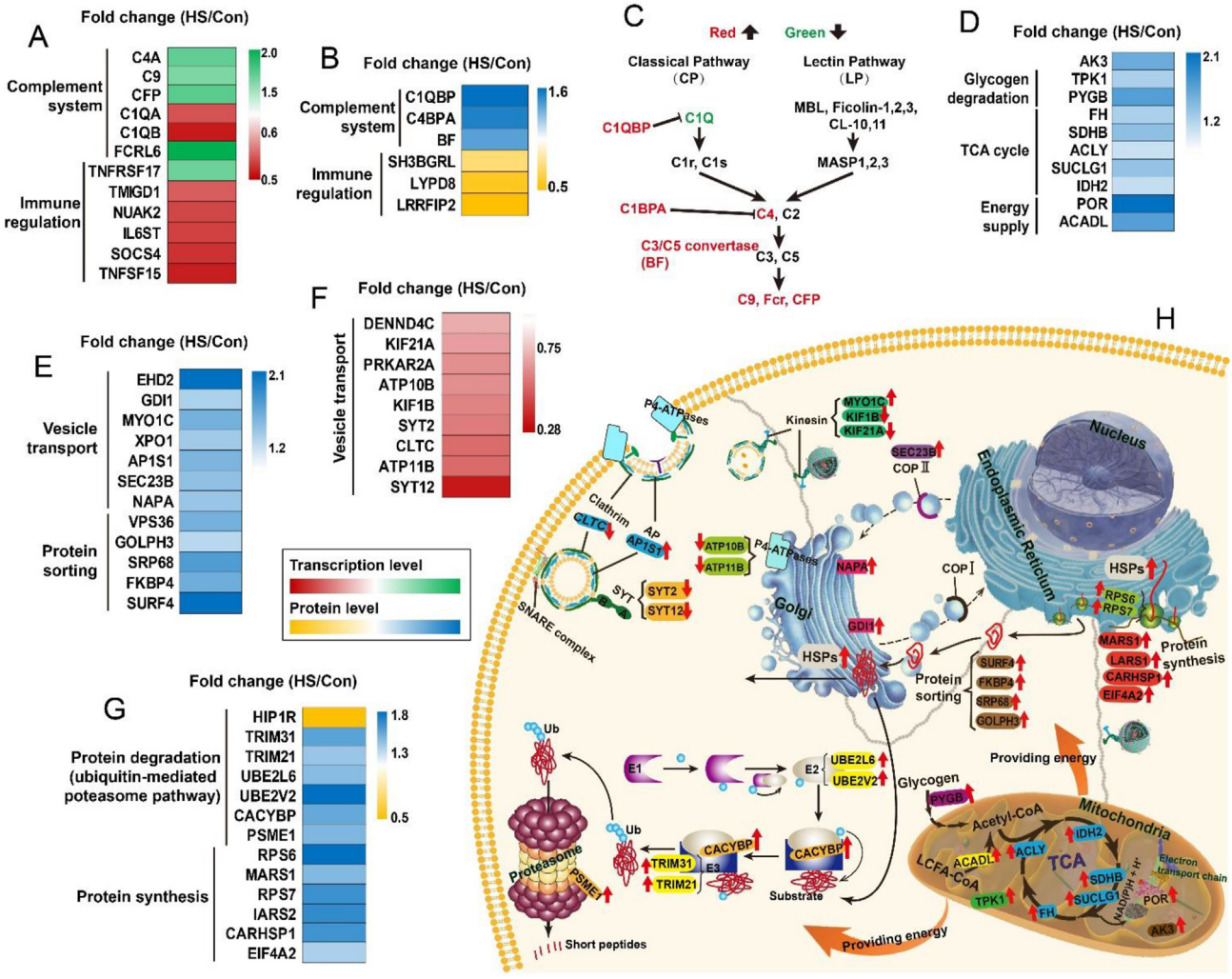

Fig. 7. Transcriptomics and proteomics revealed that chronic heat stress interfered with intestinal immunity and caused intestinal endoplasmic reticulum (ER) stress. (A and B) Fold change of differentially expressed genes or proteins related to intestinal immunity, (D) energy metabolism, (E and F) vesicle transport and protein sorting, (G) protein degradation (ubiquitin-mediated proteasome pathway) and protein synthesis; (H) the process of heat stress-induced ER stress or abnormal energy metabolism, as well as (C) complement cascade activation. (Full name of differential expression genes or proteins seen in supplementary file 1 or 3).

exerting immune defense function against external pathogens (Asano et al., 2015; Pabst et al., 2008). The expression of genes and proteins of the complement system and immune-related factors were markedly altered by chronic heat exposure as determined by transcriptomics and proteomics (Fig. 7A and B). The complement system, a critical part of the body's innate immune defense, not only contributes to local inflammation, removal and killing of pathogens, but also assists in shaping the adaptive immune response (Afshar-Kharghan, 2017). The complement cascade can be activated through 3 distinct pathways: the classical pathway (CP), the lectin pathway (LP) and the alternative pathway (AP) (Lubbers et al., 2017). Herein, heat exposure activated the complement cascade through LP instead of CP as evidenced by increased expression of C1QBP (complement C1q binding protein), BF (C3/C5 convertase), C4 (complement C4), C9, CFP (complement factor properdin), FCRL6 (Fc receptor like 6), and decreased expression of C1QA (complement C1q A chain), and C1QB (Fig. 7C). Furthermore, heat exposure reduced the proportion of Treg cells ($CD3^+$ $CD4^+$ $CD25^+$) in IEL as indicated by immunophenotyping results (Maecker et al., 2012). These findings demonstrated that heat exposure induced gut inflammation. Considering the important role of ileal PP in mucosal immunity, we further investigated the PP morphology and analyzed the immunophenotyping for PPL (Maecker et al., 2012). Chronic heat exposure decreased the size of lymphoid nodules, increased the ratio of T cells to B cells, and decreased the number of B cells, indicating that chronic heat stress might impair the development and function of PP. In addition, data from flow cytometry exhibited that chronic heat exposure increased the number of T cells in PP by upregulating the secretion of $CD4^+$ T cells, without altering the abundance of $CD8^+$ T cells. Yu et al. (2014) reported that disruption of the balance between $CD4^+$ T cell and $CD8^+$ T cell in the ileal PP node led to gut inflammation. Chronic heat exposure impaired the activation of the complement cascade response and caused imbalance of lymphocyte composition in the IEL and PPL might due to the entrance of pathogens and toxic substances into the body through the impaired gut.

Gut dysbiosis occurs when the diversity, composition and function of gut microbiota are disturbed. It is accompanied by deregulation of immune defense function and imbalance of gut homeostasis (Lee and Chang, 2021). Studies reported that the gut microbial community composition was not clearly differentiated in growing pigs after heat exposure for 3 days (Xia et al., 2022) or 7 days (Xiong et al., 2022). Similar results also found that chronic heat exposure had limited effects on the composition and abundance of gut microbes in pigs, and only a few gut microbes were affected by high ambient temperature. The majority of altered microbes were those dependent on feed intake. Of note, 10 genera of microbiota were remarkably altered in the cecum digesta of heat-stressed pigs. The potentially pathogenic bacteria, *Asteroleplasma* (Hackmann et al., 2017), *Shuttleworthia* (Lim et al., 2017), *Intestinimonas* (Chen et al., 2019), and opportunistic pathogens, *Turicibacter* and *Desulfovibrio* (Wu et al., 2018), notably increased while butyrate-producing bacteria *Coprococcus* (beneficial bacteria) (Liu et al., 2019; Reininghaus et al., 2020) markedly decreased, which contributed to the occurrence of gut inflammation. Analysis of the correlation matrix between immunophenotyping of GALT and cecal differential microbes revealed that the proportion of $CD4^+$ T cells in IEL and PPL was negatively associated with pathogenic bacteria (*Shuttleworthia*, *Turicibacter* and *Desulfovibrio*) and positively associated with *Coprococcus* (Fig. S5). By contrast, the proportion of $CD8^+$ T cells in IEL and PPL was negatively correlated with *Coprococcus*, *Defluviitaleaceae_UCG-011* and *Eubacterium_xylanophilum_group*. Similarly, the proportion of B cells in PPL was positively correlated with *Coprococcus* and negatively correlated with *Intestinimonas* and *Desulfovibro* (Fig. S5). These findings indicated that the heat stress-induced gut inflammation and alteration to immunophenotyping in GALT was mediated by intestinal microbiota dysbiosis. Among the 6 bacteria genera altered in the ileal chyme following heat exposure, the abundance of pathogenic bacteria, *Mycoplasma* (Salazar et al., 2018) and *norank_f_Erysipelotrichaceae* (Palacios-Gonzalez et al., 2020) was increased, while that of beneficial bacterium *Aeriscardovia* (Ji et al., 2020) was decreased. Most importantly, the abundance of well-established pathogens, *Escherichia_Shigella* and *Clostridium_sensu_stricto_6* (Dong et al., 2018; Fang et al., 2017; Piao et al., 2020), was significantly reduced in the ileal chyme of heat-stressed pigs. Because of the lower diversity of microbiota in the ileal chyme compared with that in ileal mucosa (Zhang et al., 2018), the decrease in pathogenic bacteria in the ileal digesta might be due to the bacterial colonization of mucosa or entry of bacteria through the unhealthy gut caused by heat exposure. This affected immune defense response in the gut, leading to activation of the intestinal complement system, alterations to the expression of immune regulation-related genes and changes to the immunophenotyping of GALT.

5. Conclusion

In this study, we demonstrated how chronic heat stress affects the transport and immune function in the pig gut by analyzing the transcriptome, proteome, microbial diversity and flow cytometry. Chronic heat stress reduced the growth performance of pigs by decreasing feed intake and diminishing the surface area of intestinal villi. Additionally, chronic heat stress had a negative impact on the gut barrier and disrupted nutrient and ion transport due to resultant ER stress. Chronic heat stress-induced ER stress increased the error rate of the protein-folding process, thereby increasing misfolded protein degradation, protein synthesis processes and vesicle transport disorder. To meet the energy demands of high energy-consuming biological processes, energy production in the mitochondrion was enhanced. In addition, chronic heat stress activated the complement cascade response in the gut mucosa, and caused an imbalance in gut lymphocytes in GALT. Chronic heat stress altered the composition of specific bacteria, increasing the number of pathogenic bacteria (e.g., *Asteroleplasma*, *Shuttleworthia*, *Mycoplasma* and so on) and decreasing beneficial bacteria (e.g., *Coprococcus* and *Aeriscardovia*), leading to alterations in gut immune function. Taken together, these results show that chronic heat stress impaired gut transport and immune function by increasing ER stress in growing pigs. These findings expand our knowledge of the molecular effects of chronic heat stress on the gut.

Author contributions

Shanlong Tang: conceptualization, Software, Formal analysis, Writing – original draft and visualization. **Jingjing Xie**: resources, Methodology, Conceptualization and supervision. **Wei Fang**: resources, Software, Formal analysis and methodology. **Xiaobin Wen**, **Chang Yin**, **Qingshi Meng**, **Ruqing Zhong** and **Liang Chen**: methodology and formal analysis. **Hongfu Zhang**: conceptualization, Supervision, Project administration and funding acquisition.

Declaration of competing interest

We declare that we have no financial and personal relationships with other people or organizations that can inappropriately influence our work, and there is no professional or other personal interest of any nature or kind in any product, service and/or company that could be construed as influencing the content of this paper.

Acknowledgements

This study was supported by the National Key R&D Program of China (2016YFD0500501), the Agricultural Science and Technology Innovation Programof China (ASTIP-IAS07) and the Seed Project of State Key Laboratory of Animal Nutrition of China (2004DA125184G2102).

Appendix A. Supplementary data

Supplementary data to this article can be found online at https://doi.org/10.1016/j.aninu.2022.08.008.

References

Afshar-Kharghan V. The role of the complement system in cancer. J Clin Invest 2017;127:780–9.
Asano K, Takahashi N, Ushiki M, Monya M, Aihara F, Kuboki E, Moriyama S, Iida M, Kitamura H, Qiu CH, Watanabe T, Tanaka M. Intestinal CD169^{+} macrophages initiate mucosal inflammation by secreting CCL8 that recruits inflammatory monocytes. Nat Commun 2015;6:7802.
Chen L, Chen DQ, Liu JR, Zhang J, Vaziri ND, Zhuang S, Chen H, Feng YL, Guo Y, Zhao YY. Unilateral ureteral obstruction causes gut microbial dysbiosis and metabolome disorders contributing to tubulointerstitial fibrosis. Exp Mol Med 2019;51:1–18.
Chi Q, Chi X, Hu X, Wang S, Zhang H, Li S. The effects of atmospheric hydrogen sulfide on peripheral blood lymphocytes of chickens: perspectives on inflammation, oxidative stress and energy metabolism. Environ Res 2018;167:1–6.
Cui Y, Gu X. Proteomic changes of the porcine small intestine in response to chronic heat stress. J Mol Endocrinol 2015;55:277–93.
Cui Y, Wang C, Hao Y, Gu X, Wang H. Chronic heat stress induces acute phase responses and serum metabolome changes in finishing pigs. Animals (Basel) 2019;9:395.
Dokladny K, Moseley PL, Ma TY. Physiologically relevant increase in temperature causes an increase in intestinal epithelial tight junction permeability. Am J Physiol Gastrointest Liver Physiol 2006;290:G204–12.
Dokladny K, Ye D, Kennedy JC, Moseley PL, Ma TY. Cellular and molecular mechanisms of heat stress-induced up-regulation of occludin protein expression: regulatory role of heat shock factor-1. Am J Pathol 2008;172:659–70.
Dong B, Liu S, Wang C, Cao Y. Effects of xylanase supplementation to wheat-based diets on growth performance, nutrient digestibility and gut microbes in weanling pigs. Asian-Australas J Anim Sci 2018;31:1491–9.
Fan H, Zhao Y, Zhu JH, Song FC, Ye JH, Wang ZY, Le JW. Thrombocytopenia as a predictor of severe acute kidney injury in patients with heat stroke, vol. 37. Renal Failure; 2015. p. 877–81.
Fang D, Shi D, Lv L, Gu S, Wu W, Chen Y, Guo J, Li A, Hu X, Guo F, Ye J, Li Y, Li L. *Bifidobacterium pseudocatenulatum* LI09 and *Bifidobacterium catenulatum* LI10 attenuate D-galactosamine-induced liver injury by modifying the gut microbiota. Sci Rep 2017;7:8770.
Gotoh T, Endo M, Oike Y. Endoplasmic reticulum stress-related inflammation and cardiovascular diseases. Int J Inflamm 2011;2011:259462.
Hackmann TJ, Ngugi DK, Firkins JL, Tao J. Genomes of rumen bacteria encode atypical pathways for fermenting hexoses to short-chain fatty acids. Environ Microbiol 2017;19:4670–83.
Hall DM, Buettner GR, Oberley LW, Xu L, Matthes RD, Gisolfi CV. Mechanisms of circulatory and intestinal barrier dysfunction during whole body hyperthermia. Am J Physiol Heart Circ Physiol 2001;280:H509–21.
Han X, Li H, Liu Q, Liu F, Arif A. Analysis of influential factors on air quality from global and local perspectives in China. Environ Pollut 2019;248:965–79.
Heneghan HM, Nazirawan F, Dorcaratto D, Fiore B, Boylan JF, Maguire D, Hoti E. Extreme heatstroke causing fulminant hepatic failure requiring liver transplantation: a case report. Transplant Proc 2014;46:2430–2.
Ji F, Zhang D, Shao Y, Yu X, Liu X, Shan D, Wang Z. Changes in the diversity and composition of gut microbiota in pigeon squabs infected with Trichomonas gallinae. Sci Rep 2020;10:19978.
Kiela PR, Ghishan FK. Ion transport in the intestine. Curr Opin Gastroenterol 2009;25:87–91.
Koch F, Thom U, Albrecht E, Weikard R, Nolte W, Kuhla B, Kuehn C. Heat stress directly impairs gut integrity and recruits distinct immune cell populations into the bovine intestine. Proc Natl Acad Sci U S A 2019;116:10333–8.
Kovats RS, Kristie LE. Heatwaves and public health in Europe. Eur J Publ Health 2006;16:592–9.
Lambert GP. Stress-induced gastrointestinal barrier dysfunction and its inflammatory effects. J Anim Sci 2009;87:101–8.
Lee M, Chang EB. Inflammatory bowel diseases (IBD) and the microbiome-searching the crime scene for clues. Gastroenterology 2021;160:524–37.
Li Y, Chen C, Cui Y. Effect of heat stress on the intestinal flora structure and alkaline phosphatase activities and mRNA expression of amino acid transporters of layer. Sci Agric Sin 2013;46:4378–87.
Lim S, Huh HJ, Lee NY, Joo EJ, Yeom JS, Lee S, Woo HY, Park H, Kwon MJ. *Robinsoniella peoriensis* Bacteremia: a second case in Korea. Ann Lab Med 2017;37:349–51.
Littmann AE, Shields RK. Whole body heat stress increases motor cortical excitability and skill acquisition in humans. Clin Neurophysiol 2016;127:1521–9.
Liu X, Zhao W, Yu D, Cheng JG, Luo Y, Wang Y, Yang ZX, Yao XP, Wu SS, Wang WY, Yang W, Li DQ, Wu YM. Effects of compound probiotics on the weight, immunity performance and fecal microbiota of forest musk deer. Sci Rep 2019;9:19146.
Liu Z, Fu Q, Tang S, Xie Y, Meng Q, Tang X, Zhang S, Zhang H, Schroyen M. Proteomics analysis of lung reveals inflammation and cell death induced by atmospheric H_2S exposure in pig. Environ Res 2020;191:110204.
Lubbers R, van Essen MF, van Kooten C, Trouw LA. Production of complement components by cells of the immune system. Clin Exp Immunol 2017;188:183–94.
Maecker HT, McCoy JP, Nussenblatt R. Standardizing immunophenotyping for the human immunology Project. Nat Rev Immunol 2012;12:191–200.
Morales A, Hernandez L, Buenabad L, Avelar E, Bernal H, Baumgard LH, Cervantes M. Effect of heat stress on the endogenous intestinal loss of amino acids in growing pigs. J Anim Sci 2016;94:165–72.
Nagao-Kitamoto H, Leslie JL, Kitamoto S, Jin C, Thomsson KA, Gillilland 3rd MG, Kuffa P, Goto Y, Jenq RR, Ishii C, Hirayama A, Seekatz AM, Martens EC, Eaton KA, Kao JY, Fukuda S, Higgins PDR, Karlsson NG, Young VB, Kamada N. Interleukin-22-mediated host glycosylation prevents *Clostridioides difficile* infection by modulating the metabolic activity of the gut microbiota. Nat Med 2020;26:608–17.
Oliveto S, Alfieri R, Miluzio A, Scagliola A, Secli RS, Gasparini P, Grosso S, Cascione L, Mutti L, Biffo S. A polysome-based microRNA screen identifies miR-24-3p as a novel promigratory miRNA in mesothelioma. Cancer Res 2018;78:5741–53.
Pabst R, Russell MW, Brandtzaeg P. Tissue distribution of lymphocytes and plasma cells and the role of the gut. Trends Immunol 2008;29:206–8.
Palacios-Gonzalez B, Ramirez-Salazar EG, Rivera-Paredez B, Quiterio M, Flores YN, Macias-Kauffer L, Moran-Ramos S, Denova-Gutierrez E, Ibarra-Gonzalez I, Vela-Amieva M, Canizales-Quinteros S, Salmeron J, Velazquez-Cruz R. A multi-omic analysis for low bone mineral density in postmenopausal women suggests a relationship between diet, metabolites, and microbiota. Microorganisms 2020;8:1630.
Pearce SC, Gabler NK, Ross JW, Escobar J, Patience JF, Rhoads RP, Baumgard LH. The effects of heat stress and plane of nutrition on metabolism in growing pigs. J Anim Sci 2013a;91:2108–18.
Pearce SC, Lonergan SM, Huff-Lonergan E, Baumgard LH, Gabler NK. Acute heat stress and reduced nutrient intake alter intestinal proteomic profile and gene expression in pigs. PLoS One 2015;10:e0143099.
Pearce SC, Mani V, Boddicker RL, Johnson JS, Weber TE, Ross JW, Rhoads RP, Baumgard LH, Gabler NK. Heat stress reduces intestinal barrier integrity and favors intestinal glucose transport in growing pigs. PLoS One 2013b;8:e70215.
Pearce SC, Mani V, Weber TE, Rhoads RP, Patience JF, Baumgard LH, Gabler NK. Heat stress and reduced plane of nutrition decreases intestinal integrity and function in pigs. J Anim Sci 2013c;91:5183–93.
Pearce SC, Sanz-Fernandez MV, Hollis JH, Baumgard LH, Gabler NK. Short-term exposure to heat stress attenuates appetite and intestinal integrity in growing pigs. J Anim Sci 2014;92:5444–54.
Piao X, Liu B, Sui X, Li S, Niu W, Zhang Q, Shi X, Cai S, Fan Y. Picroside II improves severe acute pancreatitis-induced intestinal barrier injury by inactivating oxidative and inflammatory TLR4-dependent PI3K/AKT/NF-kappaB signaling and improving gut microbiota. Oxid Med Cell Longev 2020;2020:3589497.
Reininghaus EZ, Platzer M, Kohlhammer-Dohr A, Hamm C, Morkl S, Bengesser SA, Fellendorf FT, Lahousen-Luxenberger T, Leitner-Afschar B, Schoggl H, Amberger-Otti D, Wurm W, Queissner R, Birner A, Falzberger VS, Painold A, Fitz W, Wagner-Skacel J, Brunnmayr M, Rieger A, Maget A, Unterweger R, Schwalsberger K, Reininghaus B, Lenger M, Bastiaanssen TFS, Provit Dalkner N. Supplementary probiotic treatment and vitamin B7 in depression-A randomized controlled trial. Nutrients 2020;12:3422.
Renaudeau D, Anais C, Tel L, Gourdine JL. Effect of temperature on thermal acclimation in growing pigs estimated using a nonlinear function. J Anim Sci 2010;88:3715–24.
Ron D, Walter P. Signal integration in the endoplasmic reticulum unfolded protein response. Nat Rev Mol Cell Biol 2007;8:519–29.
Rostagno MH. Effects of heat stress on the gut health of poultry. J Anim Sci 2020;98:1–9.
Salazar JK, Carstens CK, Ramachandran P, Shazer AG, Narula SS, Reed E, Ottesen A, Schill KM. Metagenomics of pasteurized and unpasteurized gouda cheese using targeted 16S rDNA sequencing. BMC Microbiol 2018;18:189.
Seelenbinder KM, Zhao LD, Hanigan MD, Hulver MW, McMillan RP, Baumgard LH, Selsby JT, Ross JW, Gabler NK, Rhoads RP. Effects of heat stress during porcine reproductive and respiratory syndrome virus infection on metabolic responses in growing pigs. J Anim Sci 2018;96:1375–87.
Slawinska A, Mendes S, Dunislawska A, Siwek M, Zampiga M, Sirri F, Meluzzi A, Tavaniello S, Maiorano G. Avian model to mitigate gut-derived immune response and oxidative stress during heat. Biosystems 2019;178:10–5.
Stocker TF. Climate change 2013: the physical science basis: working group I contribution to the fifth assessment report of the intergovernmental Panel on climate change. Computational Geometry; 2013.

Sun GX, Chen Y, Liu CP, Li S, Fu J. Effect of selenium against lead-induced damage on the gene expression of heat shock proteins and inflammatory cytokines in peripheral blood lymphocytes of chickens. Biol Trace Elem Res 2016;172:474–80.
Tang S, Xie J, Wu W, Yi B, Liu L, Zhang H. High ammonia exposure regulates lipid metabolism in the pig skeletal muscle via mTOR pathway. Sci Total Environ 2020;740:139917.
Tang S, Xie J, Zhang S, Wu W, Yi B, Zhang H. Atmospheric ammonia affects myofiber development and lipid metabolism in growing pig muscle. Animals (Basel) 2019;10:2.
Tang X, Meng Q, Gao J, Zhang S, Zhang H, Zhang M. Label-free quantitative analysis of changes in broiler liver proteins under heat stress using SWATH-MS technology. Sci Rep 2015;5:15119.
Tellez Jr G, Tellez-Isaias G, Dridi S. Heat stress and gut health in broilers: role of tight junction proteins. Adv Food Technol Nutr Sci Open J 2017;3:e1–4.
Varasteh S, Braber S, Garssen J, Fink-Gremmels J. Galacto-oligosaccharides exert a protective effect against heat stress in a Caco-2 cell model. J Funct Foods 2015;16:265–77.
Wang XJ, Feng JH, Zhang MH, Li XM, Ma DD, Chang SS. Effects of high ambient temperature on the community structure and composition of ileal microbiome of broilers. Poultry Sci 2018;97:2153–8.
Welc SS, Clanton TL, Dineen SM, Leon LR. Heat stroke activates a stress-induced cytokine response in skeletal muscle. J Appl Physiol 2013;115:1126–37.
Wu M, Wu Y, Li J, Bao Y, Guo Y, Yang W. The dynamic changes of gut microbiota in *Muc2* deficient mice. Int J Mol Sci 2018;19:2809.
Xia B, Wu W, Fang W, Wen X, Xie J, Zhang H. Heat stress-induced mucosal barrier dysfunction is potentially associated with gut microbiota dysbiosis in pigs. Anim Nutr 2022;8:289–99.
Xin H, Zhang X, Sun D, Zhang C, Hao Y, Gu X. Chronic heat stress increases insulin-like growth factor-1(IGF-1) but does not affect IGF-binding proteins in growing pigs. J Therm Biol 2018;77:122–30.
Xiong Y, Cao S, Xiao H, Wu Q, Yi H, Jiang Z, Wang L. Alterations in intestinal microbiota composition coincide with impaired intestinal morphology and dysfunctional ileal immune response in growing-finishing pigs under constant chronic heat stress. J Anim Sci Biotechnol 2022;13:1.
Yang PC, He SH, Zheng PY. Investigation into the signal transduction pathway via which heat stress impairs intestinal epithelial barrier function. J Gastroenterol Hepatol 2007;22:1823–31.
Yu XY, Zou CL, Zhou ZL, Shan T, Li DH, Cui NQ. Phasic study of intestinal homeostasis disruption in experimental intestinal obstruction. World J Gastroenterol 2014;20:8130–81308.
Zhang L, Wu W, Lee YK, Xie J, Zhang H. Spatial heterogeneity and co-occurrence of mucosal and luminal microbiome across swine intestinal tract. Front Microbiol 2018;9:48.
Zhang Y, Zhang Y, Sun K, Meng Z, Chen L. The SLC transporter in nutrient and metabolic sensing, regulation, and drug development. J Mol Cell Biol 2019;11:1–13.
Zhu L, Liao R, Wu N, Zhu G, Yang C. Heat stress mediates changes in fecal microbiome and functional pathways of laying hens. Appl Microbiol Biotechnol 2019;103:461–72.